Geophysical Research Letters

RESEARCH LETTER
10.1029/2024GL112287

Modeled Centennial Ocean Warming in the Amundsen Sea Driven by Thermodynamic Atmospheric Changes, Not Winds

K. A. Turner[1,2], K. A. Naughten[1], P. R. Holland[1], and A. C. Naveira Garabato[2]

[1]British Antarctic Survey, Cambridge, UK, [2]University of Southampton, Southampton, UK

Abstract Increased ice shelf melting caused by ocean warming in the Amundsen Sea is likely committed for the coming century. However, the drivers behind this projected ocean warming are not yet fully understood. Using a high-resolution regional model, we compare future projections of the Amundsen Sea under the RCP8.5 scenario against pre-industrial projections. The two ensembles differ measurably between 2013 and 2018, and continue to diverge under high-emissions forcing. We conduct two more experiments separating the effects of stronger, poleward-shifted winds against a warmer, wetter atmosphere (defined here as atmospheric thermodynamics). We run experiments that use RCP8.5 winds and pre-industrial thermodynamics, and vice versa. We find that atmospheric thermodynamic change modulates Circumpolar Deep Water inflow onto the shelf, making thermodynamic change the primary driver of ocean warming on the continental shelf on centennial timescales.

Plain Language Summary Increased ice loss from the West Antarctic Ice Sheet plays a significant role in determining future sea level rise. Much of this loss originates from within the Amundsen Sea sector, where the floating components of ice sheets, the ice shelves, are expected to melt more rapidly over the coming century. This increased melting is caused by warm waters entering the continental shelf and melting these ice shelves from below. While models project an increase in ocean warming over the coming century, the causes behind this warming are little understood. In this study, we untangle how climate change will affect ocean warming in the future by comparing ocean warming under high emissions to pre-industrial simulations. An anthropogenic signal in ocean warming first emerges between 2013 and 2018 in the simulations, and continues to strengthen under high-emissions forcing. We then compare the effects of stronger winds shifted southwards (wind forcing) against the impacts of a warmer, wetter atmosphere (thermodynamic forcing). We find that the thermodynamic changes are primarily responsible for the predicted Amundsen Sea warming. Under a warmer and wetter climate, the ice shelves experience an increase in the poleward flow of warmer waters at depth, leading to more melting.

Key Points:

- Ocean model experiments isolate the relative effects of atmospheric thermodynamic and wind changes on the Amundsen Sea under climate change
- Increased atmospheric warming and precipitation alter regional freshwater flux trends, accelerating the Amundsen Sea undercurrent
- Thermodynamics linked to a warmer and wetter atmosphere are the primary drivers of warming in the Amundsen Sea on centennial timescales

Supporting Information:

Supporting Information may be found in the online version of this article.

Correspondence to:

K. A. Turner,
katner33@bas.ac.uk

Citation:

Turner, K. A., Naughten, K. A., Holland, P. R., & Naveira Garabato, A. C. (2025). Modeled centennial ocean warming in the Amundsen Sea driven by thermodynamic atmospheric changes, not winds. *Geophysical Research Letters*, *52*, e2024GL112287. https://doi.org/10.1029/2024GL112287

Received 2 OCT 2024
Accepted 17 JUN 2025

Author Contributions:

Conceptualization: K. A. Naughten, P. R. Holland
Data curation: K. A. Turner
Formal analysis: K. A. Turner
Funding acquisition: K. A. Naughten, P. R. Holland, A. C. Naveira Garabato
Investigation: K. A. Turner, P. R. Holland
Methodology: K. A. Naughten
Project administration: K. A. Naughten, P. R. Holland, A. C. Naveira Garabato
Resources: K. A. Turner, K. A. Naughten, A. C. Naveira Garabato
Software: K. A. Naughten, P. R. Holland
Supervision: K. A. Naughten, P. R. Holland, A. C. Naveira Garabato

1. Introduction

The West Antarctic Ice Sheet (WAIS) is experiencing significant mass loss, contributing to sea level rise, altering the Earth's energy budget, and modulating global ocean circulation (Otosaka et al., 2022; Paolo et al., 2015; Rignot et al., 2019). A substantial proportion of this decline originates from the Amundsen Sea sector, where warm Circumpolar Deep Water (CDW) melts the ice shelves from below (Jacobs et al., 2012; Pritchard et al., 2012; Shepherd et al., 2004). There is reason to believe that anthropogenic emissions of greenhouse gases have contributed to ice shelf melting by increasing ocean temperatures, which are expected to continue warming under future emission scenarios (Figures 1a and 1c) (Naughten et al., 2022, 2023).

CDW is diverted onto the continental shelf along troughs in the bathymetry, where it is then transported to the ice shelves at depth (Figure 1b) (Assmann et al., 2013; Kimura et al., 2017; Walker et al., 2013). Its transport onto the shelf highly correlates to the Amundsen Sea Undercurrent strength, an eastward current flowing along the continental shelf break associated with the Antarctic Slope Front (ASF) (Assmann et al., 2013; Kimura et al., 2017; Walker et al., 2013). The ASF is defined by the strong slope in the pycnocline that separates the colder, fresher Winter Water, from the warmer, saltier CDW. This structure is not as pronounced in the Amundsen Sea as in other areas around Antarctica (Thompson et al., 2018), yet its coupling with the strength of the undercurrent makes it fundamental to determine future warming trends in the region (Walker et al., 2013).

Validation: K. A. Naughten, P. R. Holland
Visualization: K. A. Turner
Writing – original draft: K. A. Turner
Writing – review & editing: K. A. Turner, P. R. Holland, A. C. Naveira Garabato

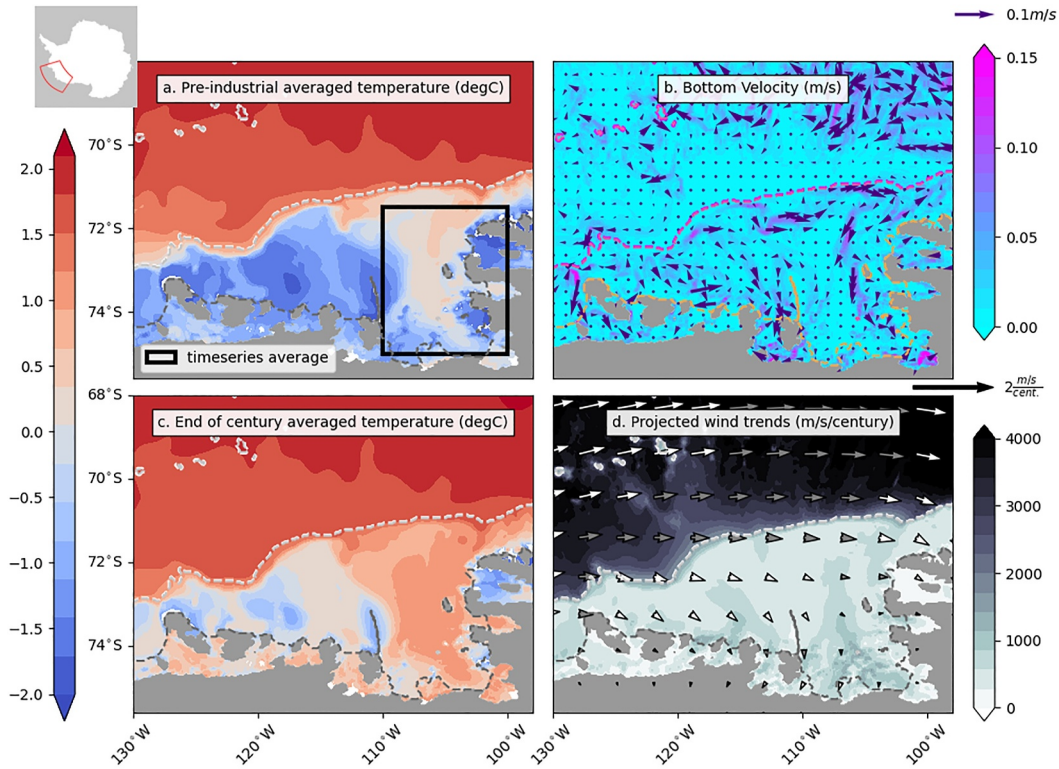

Figure 1. Average simulated potential temperature between 200 and 700 m under (a) pre-industrial and (c) RCP8.5 end of 21st-century conditions. The region outlined is studied in Figure 2. (b) Bottom ocean current velocity. (d) Bathymetry and average wind velocity trends under the RCP8.5 pathway. White arrows indicate when both velocity component trends are statistically significant to the 95% confidence level, gray shows when only one component is significant, black indicates no significance. Dashed lines represent the continental shelf (northernmost contour), and the ice shelf edge (southernmost contour). Shaded areas indicate land or grounded ice.

Some previous literature assumed that the undercurrent speed was barotropically modulated by winds at the shelf break. This hypothesis was initially backed by observations, suggesting a relationship between increased eastward wind anomalies and a strengthened eastward undercurrent (Dutrieux et al., 2014; Jenkins et al., 2016, 2018). Climate model simulations under high emissions show an increase in westerly wind anomalies over the shelf break (Figure 1) (Holland et al., 2019, 2022), leading to a theory that the barotropic component of the undercurrent would increase, driving increased ice shelf melt (Holland et al., 2019). However, Silvano et al. (2022) found that on decadal timescales, changes in the baroclinic component of the flow may outweigh the barotropic component, so that an increase in eastward wind anomalies would slow down the undercurrent instead.

Furthermore, using idealized step-change atmospheric perturbations over the Amundsen Sea, Caillet et al. (2023) investigated the reversibility of climate forcing in the region. Their study found that buoyancy fluxes are the primary driver of changes in ice shelf melting on centennial timescales, while winds make a relatively small contribution. Under this mechanism, atmospheric thermodynamic changes would alter the freshwater fluxes from sea ice and ice shelf melting, increasing ocean stratification. This process causes a cross shelf-break variation in the freshwater fluxes, steepening the ASF, and speeding up the undercurrent (Caillet et al., 2023; Jourdain et al., 2022; Si et al., 2024). Additionally, Haigh and Holland (2024) found that sea ice freshwater fluxes are responsible for the decadal variations in undercurrent strength discussed by Silvano et al. (2022).

Naughten et al. (2022, 2023) established that widespread ocean warming and increases in ice shelf melt in the Amundsen Sea are now committed for the 21st century, but did not diagnose the cause of the simulated warming. The observational record in this area is too short to detect centennial trends directly, therefore, we use high-resolution Massachusetts Institute of Technology General Circulation Model (MITgcm) simulations, a model that has been constrained using observations (Naughten et al., 2022) to perform a model-only test of the attribution. Using simulations for 1920–2100, we create four experiments to determine the dominant drivers of

warming in the Amundsen Sea over centennial timescales, separating the impacts of wind forcing from atmospheric thermodynamic forcings.

2. Methods

We use a modeling hypothesis test to distinguish the impacts of wind and thermodynamic forcing fields on the oceanographic properties of the Amundsen Sea. The study uses the MITgcm with exactly the same configuration as Naughten et al. (2022, 2023). The model domain spans 140°W–180°W and 75.5°S–62°S and has a resolution of 1/10° in longitude, and 1/10°cos θ in latitude (θ). The model has 50 vertical layers, ranging from 10 to 200 m, with the thinner layers closer to the surface (Naughten et al., 2022). The initial and boundary conditions are taken from the World Ocean Atlas (Boyer et al., 2018) and the Southern Ocean State Estimate (Verdy & Mazloff, 2017) present-day climatology.

The model is forced by atmospheric output from the CESM1 "Large Ensemble" (LENS) (Kay et al., 2015), which provides near-surface zonal and meridional winds, temperature, precipitation, sea-level pressure, humidity, and long- and short-wave radiation fluxes. The LENS data set provides the atmospheric forcing fields for three categories of simulation: pre-industrial control, historical period from 1920 to 2005, and high greenhouse gas forcing from 2006 to 2100. The latter period uses the IPCC Representative Concentration Pathway (RCP) 8.5 as an MITgcm forcing field, representing an upper bound of projected high-emissions forcing. While the RCP8.5 pathway is often criticized for posing an extreme forecast for the future (Hausfather & Peters, 2020), it allows for a clear signal distinction between anthropogenic forcing (greenhouse gases, ozone depletion, aerosols, land use change) and internal variability, requiring fewer ensemble members. Using the upper bound in climate predictions also has the advantage of illustrating the model transition through other levels of anthropogenic forcing.

Ensembles of simulations forced by historical and high-emissions future CESM1 data sets have been described in previous literature (Holland et al., 2022; Naughten et al., 2022, 2023), while a set of simulations forced by a pre-industrial control simulation data set was new to this study. We take the 1,700 years of pre-industrial simulation from CESM1, and split these into nine ensemble members comprised of 181 years each, to match the historical and high-emissions data sets.

As detailed in Naughten et al. (2022, 2023), while the model generally agrees with observations, it tends to over-simulate deep convective events; this model bias was shown not to affect the estimated warming trends for the region.

Using the data sets described above, this study creates four experiments, each comprising nine ensemble members spanning 181 years (from 1920 to 2100). We use the pre-industrial atmospheric forcing fields as our control (*NONE* experiment) and compare it to three experiments, each with different atmospheric forcing fields:

- *ALL*: atmospheric forcing fields are taken from the historical + RCP8.5 pathway scenario. This experiment represents warming under complete high-emissions forcing.
- *WIND*: MITgcm is forced by historical + RCP8.5 zonal and meridional surface winds, while the atmospheric thermodynamic forcing fields (surface temperature, humidity, precipitation, sea-level pressure, and long- and short-wave radiation) are taken from the pre-industrial ensemble, isolating the impact of changes in wind patterns on the climate system.
- *THERMO*: atmospheric thermodynamic forcing fields are taken from the historical + RCP8.5 scenario, while winds are taken from the pre-industrial scenario. This experiment isolates the impact of changes to atmospheric thermodynamic variables on the climate system.

To ensure consistency with previous studies, all four experiments were initialized from a set of initial conditions generated by a 30-year spin-up using the RCP8.5 LENS simulations from 1920 to 1949 as in Naughten et al. (2023). When perturbing the winds in the WIND ensemble, we perturb both the wind in the momentum flux calculation (therefore, the ocean and sea-ice surface friction) and the wind seen by latent and sensible heat fluxes in the bulk formulae. This choice is made so that between the WIND and THERMO ensembles we have captured all the surface forcing perturbations occurring in ALL. Each ensemble member of each experiment was matched to the corresponding spin-up ensemble member. All experiments use present-day climatology boundary conditions as described in Naughten et al. (2023).

Our experiments use present-day climatology boundaries, which exclude the influence of a changing climate further afield (Gómez-Valdivia et al., 2023; Nakayama et al., 2014; Naughten et al., 2022; Prend et al., 2024). To assess the impact of transient boundaries, we re-ran the ALL and THERMO experiments with boundary conditions which evolve in response to climate change occurring outside of the modeled region (Texts S1 and S2 in Supporting Information S1).

2.1. Analysis of Non-Linearities

The separate wind-only and thermodynamic-only experiments are purely conceptual, as winds are strongly interlinked with thermodynamic atmospheric conditions. The difference in origin in the forcing fields also leads to a mismatch in variability. However, we argue that these model experiments help us understand how changes to individual atmospheric forcing field variables govern future ocean warming in a controlled environment. The extent to which these experiments are useful depends upon how well the total response to anthropogenic forcing arises as a linear sum of the wind-only and thermodynamic-only responses.

In ALL, we expect the total oceanographic response to arise through a nonlinear interaction between wind and thermodynamic forcing fields, complicating our interpretation of the experiments. We quantify this issue by defining non-linearity as the residual of the total forced change in any output variable (such as ocean warming) that the linear sum of wind-only and thermodynamic-only changes does not explain:

residual = (ALL - NONE) - (WIND - NONE) - (THERMO - NONE)

In a linear system, we would expect the residual to equal zero. However, in the real Amundsen Sea, we expect to see non-linearities develop with time due to the mismatch between the forcing fields.

3. Results

3.1. Warming Trends Under the Four Experiments

Figure 2 illustrates the evolution of ocean temperatures over the continental shelf for our four experiments: NONE, ALL, WIND, and THERMO. The depth was chosen to approximate the depth of the ice shelf cavities. The figure shows potential temperature anomalies relative to the mean of the control experiment (NONE).

As expected, the NONE temperatures remain steady on average, with frequent cold ocean convective events that are a feature of this model prior to the onset of an anthropogenic signal in ocean warming (Naughten et al., 2022). ALL features an ocean warming that reaches 1.5°C by the end of the 21st century, with a significantly decreased variability between ensemble members caused by a shutdown in ocean convective events (Naughten et al., 2023). From this point, we define the anthropogenic forcing response as the ensemble-mean difference between ALL and NONE.

Highlighted years indicate when two experiment ensembles diverge significantly at 95% confidence (Text S2 in Supporting Information S1). According to our definition of divergence, the ALL experiment diverges from NONE in 2018 in our simulations, implying that the influence of anthropogenic forcing exists in the present day. This result varies slightly when using transient boundaries, moving the year of divergence to 2013. This is a new result that is only possible due to our pre-industrial simulations (Text S3 in Supporting Information S1). This result is subject to substantial structural uncertainty arising from our modeling setup and selected climate model forcing fields, which is elaborated upon in the Discussion below.

Throughout the experiment, THERMO remains similar to ALL, diverging from NONE in 1997 and never diverges from ALL. By 2100, the THERMO experiment mean has warmed nearly as much as ALL (only 0.25°C cooler) and shows a similar decrease in variability. WIND, however, never diverges significantly from NONE, indicating that the influence of wind changes is much smaller than assumed in previous literature. Intra-ensemble variability remains high in WIND, with a small and statistically insignificant cooling compared to NONE.

Non-linear effects are reported in Figure 2 as the dashed line, starting from the first year of divergence. By the end of the simulation, non-linear interactions between winds and thermodynamic forcing account for approximately one-third of the predicted warming. This non-linearity makes up the 0.25°C difference between ALL and THERMO, and the 0.25°C cooling between WIND and NONE. Thus, the sum of our WIND and THERMO experiments cannot explain a predicted 0.5°C of the total warming reported in the ALL experiment.

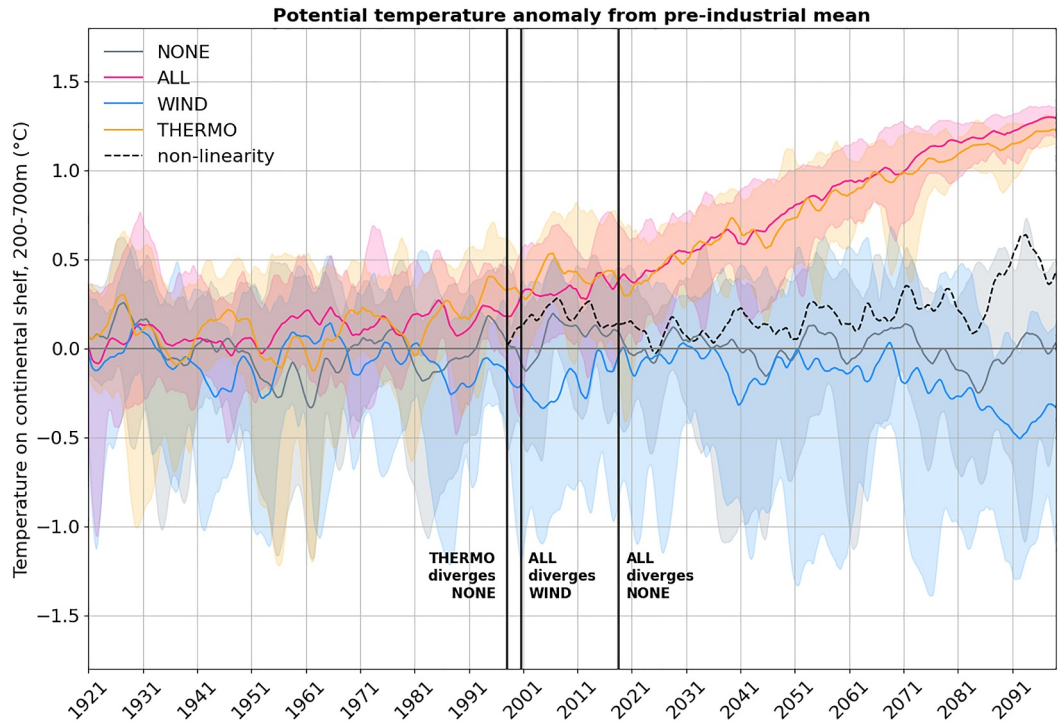

Figure 2. Potential temperature anomalies relative to the pre-industrial mean between 200 and 700 m on the continental shelf between 130°W and 95°W and 67°S and 75°S, as highlighted in Figure 1a. A 2-year rolling mean is applied. The shaded area represents the ensemble range, while the solid line is the ensemble mean. The dashed black line represents the calculated non-linearity. The years of divergence between the various experiments are highlighted in the vertical lines.

Figure 3 displays the spatial variation in warming between our experiments by 2100. The first column shows the calculated end-of-21st-century climatologies for each experiment, while the other columns show the experiment anomalies with respect to NONE and ALL. ALL and THERMO show significant warming on the continental shelf by the end of the 21st century, indicating an increased presence of CDW.

Within these climatologies, the differences between ALL and THERMO are significant, but small compared to their anomaly with respect to NONE. The WIND experiment shows some significant cooling compared to NONE, around 0.8°C at its coolest in the ice shelf cavities. This could signal increasing wind-driven convection events caused by strong winds and a cold pre-industrial atmosphere (Text S3 in Supporting Information S1). In the top right corner of Figure 3 we observe the non-linear effects, which are mainly concentrated on the continental shelf and are strongest near the ice shelves, where we observe the overall 1.5°C warming anomaly.

These results imply that thermodynamic atmospheric forcing accounts for most of the predicted ocean warming under anthropogenic forcing. The THERMO experiment shows a significant influx of CDW similar to that in ALL, while WIND remains statistically indistinguishable from NONE. We now explain how the thermodynamic atmospheric forcing drives this increased CDW influx.

3.2. Spatial Variations in Freshwater Fluxes on Centennial Timescales

The left column of Figure 4 illustrates the freshwater flux trends from 1920 to 2100. Positive values indicate an influx of freshwater into the ocean, decreasing salinity. In Figure 4, ALL and THERMO show the same pattern of increased freshening on the continental shelf and decreased freshening north of the shelf break. These patterns are primarily caused by sea ice melting and freezing changes driven by high thermodynamic forcing with a small contribution to the north made by increases in precipitation over open water (not shown).

Around Antarctica, sea ice generally forms close to the continent and is then advected north until it reaches a region where it is no longer thermodynamically sustainable and melts (Abernathey et al., 2016; Holland & Kimura, 2016). We observe an analogous sea ice conveyor pattern within the Amundsen Sea (Text S4 in

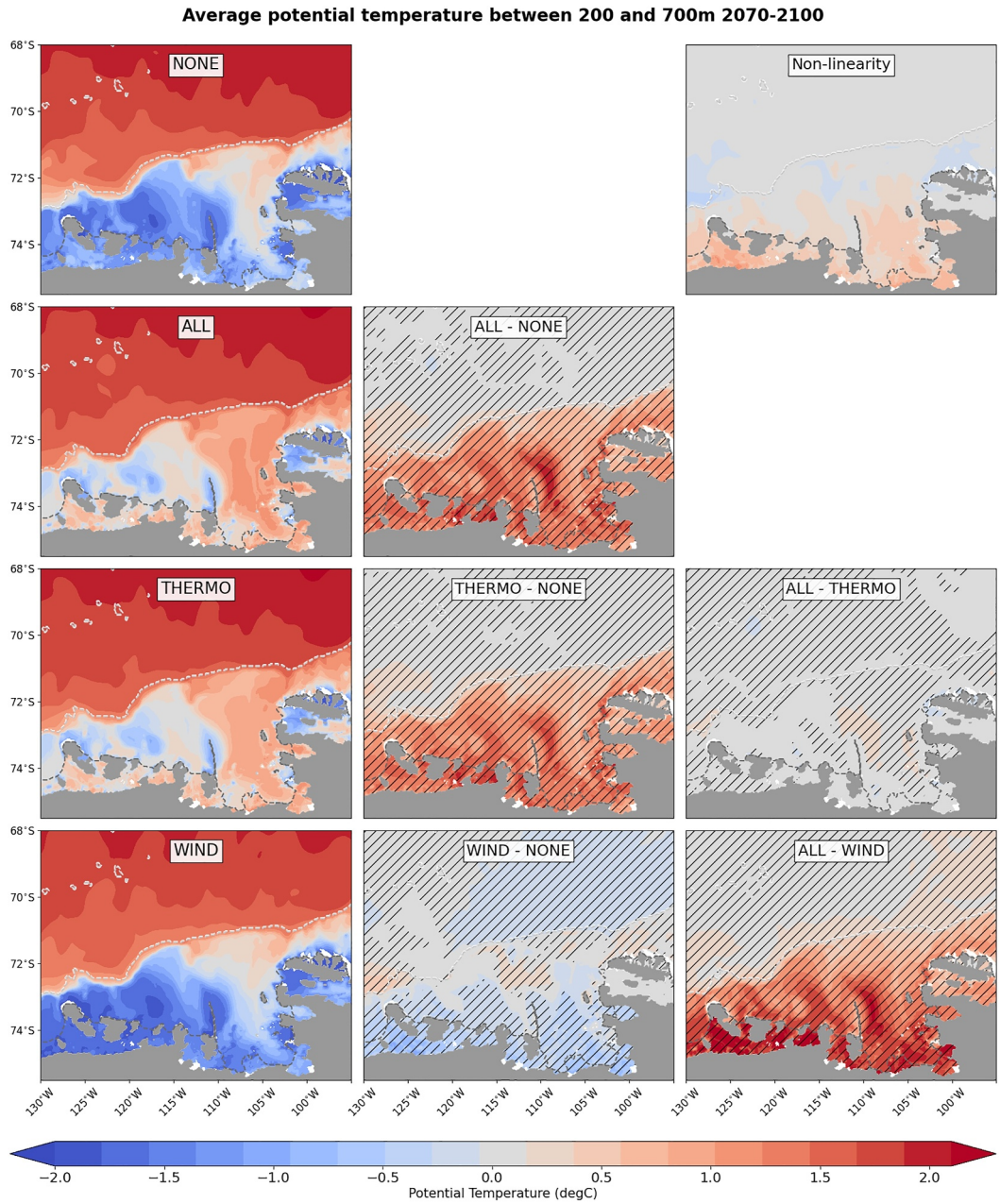

Figure 3. First column: average potential temperature between 200 and 700 m for 2070–2100. The following columns are anomalies from NONE (second column) and ALL (third column). The shading represents areas where the difference between experiments is significant.

Supporting Information S1). This conveyor-style mechanism increases salinity on the continental shelf through brine rejection from sea-ice formation, freshening the ocean north of the shelf break as the sea ice is melted.

From the 1990s, in both ALL and THERMO, the increase in atmospheric warming leads to a substantial decline in the sea ice in the region (Figure S4 in Supporting Information S1), much as shown under the idealized forcing of Caillet et al. (2023). This reduces the sea ice formation on the shelf, leading to a freshening there (Figure 4). The decline in sea ice also reduces ice export northwards, causing reduced freshening north of the shelf break as melt rates decrease.

The WIND experiment weakly shows the reverse trend. The increase in ice export and convection in WIND cools and salinifies the water on the continental shelf, as discussed in the previous section, particularly near the coast.

10.1029/2024GL112287

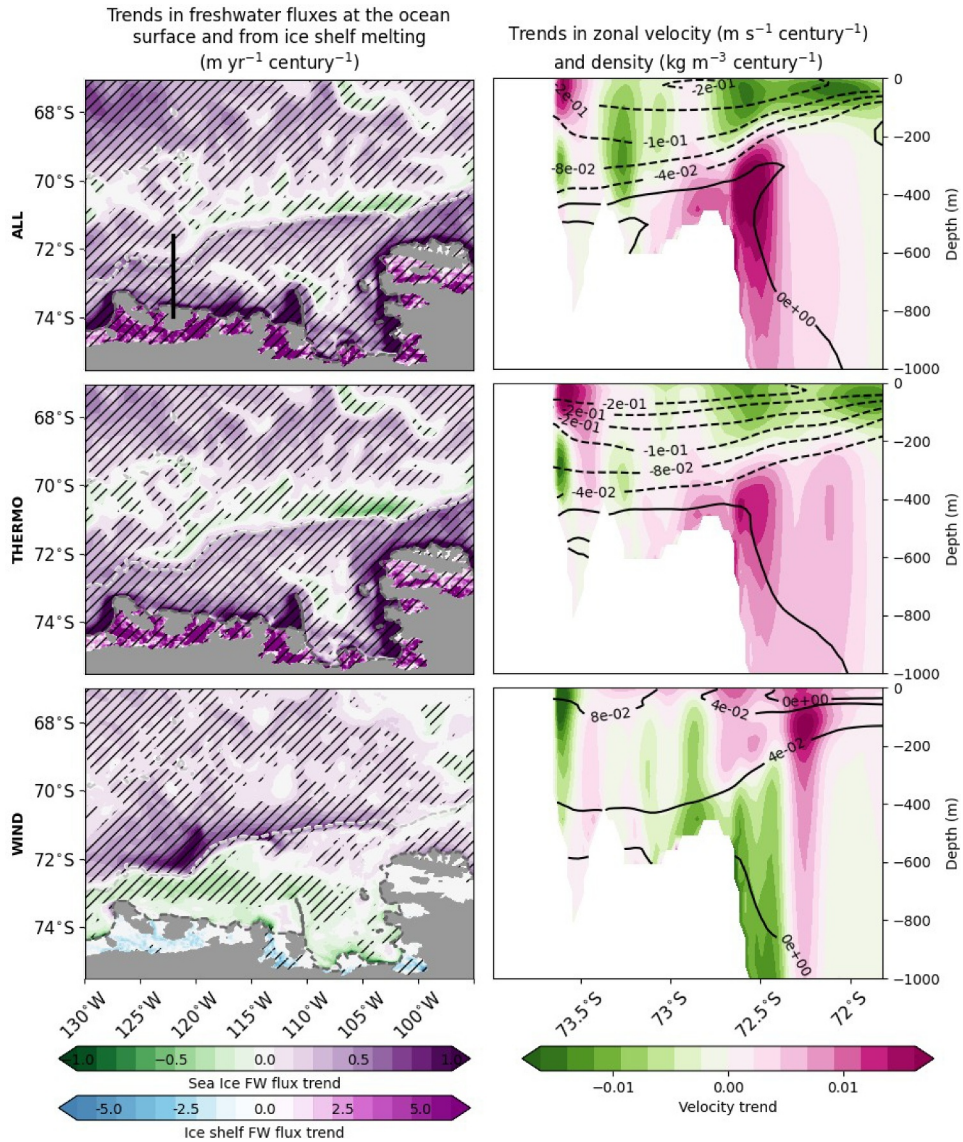

Figure 4. Left: trends in the freshwater fluxes at the ocean surface and from ice shelf melting. A positive value indicates a decrease in salinity. Note that the sea-ice and ice shelf freshwater outputs are shown on different scales. Shaded areas indicate where the experiment trends were significantly different from NONE. Right: trends in density (contours) and zonal velocity (colors) along a meridional cross-section at 118°W as highlighted on the top-left by the black line. Trends are calculated from 1920 to 2100.

This creates a small and statistically insignificant salinifying trend on the continental shelf (Figure 4). However, a significant freshening occurs north of the shelf break, which is likely due to the increased sea-ice advection here.

In summary, ALL and THERMO experience decreased sea ice cover, reducing the sea-ice conveyor of freshwater northwards off the shelf, as found by Caillet et al. (2023) under idealized forcing. This freshens the shelf and increases salinity off the shelf. Shelf freshening is enhanced by increased ice shelf melting. This result expands on the findings from Haigh and Holland (2024) on decadal timescales to centennial timescales. Here thermodynamic atmospheric changes result in a horizontal variance in the freshwater fluxes between the continental shelf and deep ocean.

3.3. Trends in the Amundsen Sea Undercurrent

The right column of Figure 4 shows a cross-section at 118°W of zonal velocity trends and density over the model run period. Dashed lines represent negative density trends, and positive velocity values indicate an increase in the flow out of the page (eastward flow).

In polar regions, salinity, rather than temperature, determines the water mass density. Therefore, the freshening trends in ALL and THERMO reported in the previous section can be translated into the decrease in surface density on the continental shelf in Figure 4. Due to the spatial pattern of the freshwater flux trend, changes in density cause an increase in the density gradient over the continental shelf, strengthening the ASF.

The strengthened ASF in ALL and THERMO instigates a geostrophic response in the undercurrent velocity (Text S5 in Supporting Information S1), increasing the shear over the shelf break and speeding up the westward surface current and eastward undercurrent. This acceleration enhances CDW transport toward the continental shelf, as implied by the slight increase in density at depth on the continental shelf, and the warming reported in Figure 3. All these processes work to increase ice shelf melt. This increase is shown on the left of Figure 4, where there is a clear increase in the melt trend across all ice shelves. This process introduces more freshwater into the system, instigating a positive feedback loop (Haigh & Holland, 2024).

The freshwater patterns in the WIND experiment lead to increasing surface density that reduces with depth. This signal is again strongest on the continental shelf, weakening the ASF and undercurrent. This slowdown in the undercurrent under an eastward wind trend is as predicted on decadal scales by Silvano et al. (2022).

4. Discussion

Using MITgcm, we examine the effects and drivers of anthropogenic climate change on ocean warming in the Amundsen Sea on centennial timescales. We find that an ensemble of simulations with anthropogenic forcing (ALL) diverges from a pre-industrial ensemble (NONE) between 2013 and 2018, depending on the boundary conditions used. This implies that, in our model configuration, Amundsen Sea temperatures did not appear to be influenced by anthropogenic forcing over the historical period. However, this influence becomes clearer and separate from internal variability in the contemporary period and will continue to grow. We believe this is the first time such a test has been reported.

This result is subject to limitations and requires further study. Our forcing fields are taken from one climate model, CESM1, and are subject to that model's climate sensitivity, which is known to be high (Bacmeister et al., 2020), and our study's model biases which are documented in the Methods section (Naughten et al., 2022, 2023). Furthermore, these experiments are run using a single regional model and do not consider far-field effects under a changing climate, which are known to be important (Gómez-Valdivia et al., 2023; Naughten et al., 2023). Recent proxy-based reconstructions of the atmosphere in this area (Dalaiden et al., 2024; O'Connor et al., 2021) show that CESM1 does a reasonably good job of replicating large scale wind and sea level pressure trends over the historical period. Furthermore, previous validations of this ocean model configuration (Holland et al., 2019; Naughten et al., 2022, 2023) demonstrate that it can reproduce the regional ocean state and variability. We therefore consider the simulated ocean response presented here to be a physically plausible consequence to the forcing experiments applied, however, future studies would certainly benefit from considering a larger ensemble of models to examine how these results are influenced by climate model structure.

We establish that THERMO replicates the processes occurring in ALL, appearing to be primarily driven by trends in freshwater fluxes from sea ice trends. Our experiments show that before the 2010s, the simulations are strongly influenced by decadal variability as described in previous studies (Haigh & Holland, 2024; Jenkins et al., 2016) (Text S4 in Supporting Information S1), after which, atmospheric thermodynamics take over, and begin decreasing sea ice production, as described in Caillet et al. (2023)'s idealized study. This creates the spatial variation in trends in freshwater fluxes shown in ALL and THERMO in Figure 4. These changes increase the cross-slope density differences, strengthening the ASF, and accelerating the undercurrent. The undercurrent then increases the transport of CDW onto the shelf, which warms the waters at depth, increasing the ice shelf melting.

As defined in the methods section, THERMO comprises surface temperature, humidity, precipitation, sea-level pressure, and radiative forcing. These variables are expected to change in response to climate change. However,

the magnitude and certainty of these changes vary among these variables (Text S6 in Supporting Information S1) so we expect their relative impact on ocean warming to be complex.

Future research should build on this study by employing the methods described to untangle the individual effects of these variables. While this approach would provide more detailed insights, it would also increase the complexity of the analysis. A significantly larger number of simulation ensembles would be required, and the non-linear interactions among variables would become increasingly challenging to interpret.

Anthropogenically forced winds alone cannot explain these patterns. In our WIND experiment convection increases under strong winds and cool atmosphere, leading to cooling at depth (Figure S3 in Supporting Information S1). The WIND experiment also shows that on centennial timescales wind forcing works via similar mechanisms to those described by Silvano et al. (2022), in which stronger eastward winds decrease the cross-shelf density gradient and baroclinically decelerate the undercurrent. The density trends appear similar to those observed by Haigh and Holland (2024) on decadal scales, with a clear opposite sign in trend north of the shelf break. However, our WIND signals remain small or statistically insignificant, indicating that the overall influence of wind forcing is minimal.

5. Conclusions

Naughten et al. (2023) present a challenging prognosis for the future of the Amundsen Sea glaciers, highlighting the ocean warming expected during the current century. The present study investigates the root causes behind these projections. Our experiment builds upon findings from previous studies investigating the influence of atmospheric forcing on decadal scales (Haigh & Holland, 2024; Silvano et al., 2022) or in idealized settings (Caillet et al., 2023; Jourdain et al., 2022; Si et al., 2024). Using a high-resolution regional model under atmospheric forcing from a climate model, we find that atmospheric thermodynamic changes are the dominant driver of warming in the Amundsen Sea on centennial time scales. These trends are initiated by changes in sea ice formation and then enhanced by a positive feedback loop, whereby an increase in ice shelf melt leads to increased warming, which increases melt. This suggests the need for an enhanced research focus on future changes in the thermodynamic forcing of the Amundsen Sea, including the correct implementation of buoyancy fluxes from changes in ice shelf and iceberg melting.

Data Availability Statement

The analysis code used is publicly accessible via zenodo (Turner, 2024). A processed version of the output is available through the Polar Data Centre (Turner & Naughten, 2024). Due to its large size, the full unprocessed data set is not hosted on a public-facing server, but subsets can be transferred on an individual basis as required. To obtain model output beyond the publicly accessible version, please contact the corresponding author.

Acknowledgments

We thank the CESM Climate Variability and Change Working Group for producing the CESM1 ensembles for community use. The authors benefited from helpful discussions with M. Haigh, A. Styles, and T. Bilge. This work used computational resources provided by the ARCHER2 UK National Supercomputing Service (http://www.archer.ac.uk/). This research used computing hours from the UKRI-JSPS project "Quantifying Human Influence on Ocean Melting of the West Antarctic Ice Sheet" budget (NE/S011994/1, K.A.N., P.R.H.). K. Turner thanks funding from the NERC-funded Doctoral Training Partnership INSPIRE (NE/S007210/1). K. Naughten acknowledges funding from TerraFIRMA (NE/W004895/1). P. Holland acknowledges funding from AnthroFAIL (NE/X000397/1). A. Naveira Garabato acknowledges U.K. Research and Innovation guarantee funding for a European Research Council Advanced Grant (EP/X025136/1).

References

Abernathey, R. P., Cerovecki, I., Holland, P. R., Newsom, E., Mazloff, M., & Talley, L. D. (2016). Water-mass transformation by sea ice in the upper branch of the Southern Ocean overturning. *Nature Geoscience*, *9*(8), 596–601. https://doi.org/10.1038/ngeo2749

Assmann, K. M., Jenkins, A., Shoosmith, D. R., Walker, D. P., Jacobs, S. S., & Nicholls, K. W. (2013). Variability of circumpolar deep water transport onto the Amundsen Sea continental shelf through a shelf break trough. *Journal of Geophysical Research: Oceans*, *118*(12), 6603–6620. https://doi.org/10.1002/2013JC008871

Bacmeister, J. T., Hannay, C., Medeiros, B., Gettelman, A., Neale, R., Fredriksen, H.-B., et al. (2020). CO_2 increase experiments using the CESM: Relationship to climate sensitivity and comparison of CESM1 to CESM2. *Journal of Advances in Modeling Earth Systems*, *12*(11), e2020MS002120. https://doi.org/10.1029/2020ms002120

Boyer, T. P., García, H. E., Locarnini, R. A., Zweng, M. M., Mishonov, A. V., Reagan, J. R., et al. (2018). World Ocean Atlas.

Caillet, J., Jourdain, N. C., Mathiot, P., Hellmer, H. H., & Mouginot, J. (2023). Drivers and reversibility of abrupt ocean state transitions in the Amundsen Sea, Antarctica. *Journal of Geophysical Research: Oceans*, *128*(1), e2022JC018929. https://doi.org/10.1029/2022JC018929

Dalaiden, Q., Abram, N. J., Goosse, H., Holland, P. R., O'Connor, G. K., & Topál, D. (2024). Multi-decadal variability of Amundsen Sea low controlled by natural tropical and anthropogenic drivers. *Geophysical Research Letters*, *51*(16), e2024GL109137. https://doi.org/10.1029/2024GL109137

Dutrieux, P., De Rydt, J., Jenkins, A., Holland, P. R., Ha, H. K., Lee, S. H., et al. (2014). Strong sensitivity of Pine Island ice-shelf melting to climatic variability. *Science*, *343*(6167), 174–178. https://doi.org/10.1126/science.1244341

Gómez-Valdivia, F., Holland, P. R., Siahaan, A., Dutrieux, P., & Young, E. (2023). Projected west Antarctic Ocean warming caused by an expansion of the ross gyre. *Geophysical Research Letters*, *50*(6), e2023GL102978. https://doi.org/10.1029/2023GL102978

Haigh, M., & Holland, P. R. (2024). Decadal variability of ice-shelf melting in the Amundsen Sea driven by sea-ice freshwater fluxes. *Authorea Preprints*, *51*(9), e2024GL108406. https://doi.org/10.1029/2024gl108406

Hausfather, Z., & Peters, G. P. (2020). Emissions–the 'business as usual' story is misleading. *Nature*, *577*(7792), 618–620. https://doi.org/10.1038/d41586-020-00177-3

Holland, P. R., Bracegirdle, T. J., Dutrieux, P., Jenkins, A., & Steig, E. J. (2019). West Antarctic ice loss influenced by internal climate variability and anthropogenic forcing. *Nature Geoscience*, *12*(9), 718–724. https://doi.org/10.1038/s41561-019-0420-9

Holland, P. R., & Kimura, N. (2016). Observed concentration budgets of Arctic and Antarctic sea ice. *Journal of Climate*, *29*(14), 5241–5249. https://doi.org/10.1175/jcli-d-16-0121.1

Holland, P. R., O'Connor, G. K., Bracegirdle, T. J., Dutrieux, P., Naughten, K. A., Steig, E. J., et al. (2022). Anthropogenic and internal drivers of wind changes over the Amundsen Sea, West Antarctica, during the 20th and 21st centuries. *The Cryosphere*, *16*(12), 5085–5105. https://doi.org/10.5194/tc-16-5085-2022

Jacobs, S., Jenkins, A., Hellmer, H., Giulivi, C., Nitsche, F., Huber, B., & Guerrero, R. (2012). The Amundsen Sea and the Antarctic ice sheet. *Oceanography*, *25*(3), 154–163. https://doi.org/10.5670/oceanog.2012.90

Jenkins, A., Dutrieux, P., Jacobs, S., Steig, E. J., Gudmundsson, G. H., Smith, J., & Heywood, K. J. (2016). Decadal ocean forcing and Antarctic ice sheet response: Lessons from the Amundsen Sea. *Oceanography*, *29*(4), 106–117. https://doi.org/10.5670/oceanog.2016.103

Jenkins, A., Shoosmith, D., Dutrieux, P., Jacobs, S., Kim, T. W., Lee, S. H., et al. (2018). West Antarctic ice sheet retreat in the Amundsen Sea driven by decadal oceanic variability. *Nature Geoscience*, *11*(10), 733–738. https://doi.org/10.1038/s41561-018-0207-4

Jourdain, N. C., Mathiot, P., Burgard, C., Caillet, J., & Kittel, C. (2022). Ice shelf basal melt rates in the Amundsen Sea at the end of the 21st century. *Geophysical Research Letters*, *49*(22), e2022GL100629. https://doi.org/10.1029/2022GL100629

Kay, J. E., Deser, C., Phillips, A., Mai, A., Hannay, C., Strand, G., et al. (2015). The community Earth system model (CESM) large ensemble project: A community resource for studying climate change in the presence of internal climate variability. *Bulletin of the American Meteorological Society*, *96*(8), 1333–1349. https://doi.org/10.1175/bams-d-13-00255.1

Kimura, S., Jenkins, A., Regan, H., Holland, P. R., Assmann, K. M., Whitt, D. B., et al. (2017). Oceanographic controls on the variability of ice-shelf basal melting and circulation of glacial meltwater in the Amundsen Sea Embayment, Antarctica. *Journal of Geophysical Research: Oceans*, *122*(12), 10131–10155. https://doi.org/10.1002/2017jc012926

Nakayama, Y., Timmermann, R., Rodehacke, C. B., Schröder, M., & Hellmer, H. H. (2014). Modeling the spreading of glacial meltwater from the Amundsen and Bellingshausen Seas. *Geophysical Research Letters*, *41*(22), 7942–7949. https://doi.org/10.1002/2014gl061600

Naughten, K., Holland, P. R., & De Rydt, J. (2023). Unavoidable future increase in West Antarctic ice-shelf melting over the twenty-first century. *Nature Climate Change*, *13*(11), 1222–1228. https://doi.org/10.1038/s41558-023-01818-x

Naughten, K., Holland, P. R., Dutrieux, P., Kimura, S., Bett, D. T., & Jenkins, A. (2022). Simulated twentieth-century ocean warming in the Amundsen Sea, west Antarctica. *Geophysical Research Letters*, *49*(5), e2021GL094566. https://doi.org/10.1029/2021GL094566

O'Connor, G. K., Steig, E. J., & Hakim, G. J. (2021). Strengthening southern hemisphere westerlies and Amundsen Sea low deepening over the 20th century revealed by proxy-data assimilation. *Geophysical Research Letters*, *48*(24), e2021GL095999. https://doi.org/10.1029/2021gl095999

Otosaka, I. N., Shepherd, A., Ivins, E. R., Schlegel, N.-J., Amory, C., van den Broeke, M., et al. (2022). Mass balance of the Greenland and Antarctic ice sheets from 1992 to 2020. *Earth System Science Data Discussions*, *2022*, 1–33. https://doi.org/10.5194/egusphere-egu22-10065

Paolo, F. S., Fricker, H. A., & Padman, L. (2015). Volume loss from Antarctic ice shelves is accelerating. *Science*, *348*(6232), 327–331. https://doi.org/10.1126/science.aaa0940

Prend, C. J., MacGilchrist, G. A., Manucharyan, G. E., Pang, R. Q., Moorman, R., Thompson, A. F., et al. (2024). Ross Gyre variability modulates oceanic heat supply toward the West Antarctic continental shelf. *Communications Earth & Environment*, *5*(1), 1–10. https://doi.org/10.1038/s43247-024-01207-y

Pritchard, H. D., Ligtenberg, S. R. M., Fricker, H. A., Vaughan, D. G., van den Broeke, M. R., & Padman, L. (2012). Antarctic ice-sheet loss driven by basal melting of ice shelves. *Nature*, *484*(7395), 502–505. https://doi.org/10.1038/nature10968

Rignot, E., Mouginot, J., Scheuchl, B., Van Den Broeke, M., Van Wessem, M. J., & Morlighem, M. (2019). Four decades of Antarctic ice sheet mass balance from 1979–2017. *Proceedings of the National Academy of Sciences of the United States of America*, *116*(4), 1095–1103. https://doi.org/10.1073/pnas.1812883116

Shepherd, A., Wingham, D., & Rignot, E. (2004). Warm ocean is eroding West Antarctic ice sheet. *Geophysical Research Letters*, *31*(23), L23402. https://doi.org/10.1029/2004gl021106

Si, Y., Stewart, A. L., Silvano, A., & Naveira Garabato, A. C. (2024). Antarctic slope undercurrent and onshore heat transport driven by ice shelf melting. *Science Advances*, *10*(16), eadl0601. https://doi.org/10.1126/sciadv.adl0601

Silvano, A., Holland, P. R., Naughten, K. A., Dragomir, O., Dutrieux, P., Jenkins, A., et al. (2022). Baroclinic ocean response to climate forcing regulates decadal variability of ice-shelf melting in the Amundsen Sea. *Geophysical Research Letters*, *49*(24), e2022GL100646. https://doi.org/10.1029/2022GL100646

Thompson, A. F., Stewart, A. L., Spence, P., & Heywood, K. J. (2018). The Antarctic slope current in a changing. *Climate*, *56*(4), 741–770. https://doi.org/10.1029/2018RG000624

Turner, K. A. (2024). Code and dataset acompanying "modelled centennial ocean warming in the Amundsen Sea driven by thermodynamic atmospheric changes, not winds" (1.0) [Software]. *Zenodo*. https://doi.org/10.5281/zenodo.13880617

Turner, K. A., & Naughten, K. A. (2024). Analysis output of the MITgcm ocean model data for the Amundsen Sea (1920 to 2100) (version 1.0). [Dataset]. *NERC EDS UK Polar Data Centre*. https://doi.org/10.5285/8A2B18EB-4720-4A40-A52A-B8F571B26B28

Verdy, A., & Mazloff, M. R. (2017). A data assimilating model for estimating Southern Ocean biogeochemistry. *Journal of Geophysical Research: Oceans*, *122*(9), 6968–6988. https://doi.org/10.1002/2016jc012650

Walker, D. P., Jenkins, A., Assmann, K. M., Shoosmith, D. R., & Brandon, M. A. (2013). Oceanographic observations at the shelf break of the Amundsen Sea, Antarctica. *Journal of Geophysical Research: Oceans*, *118*(6), 2906–2918. https://doi.org/10.1002/jgrc.20212

References From the Supporting Information

Lamarque, J.-F., Bond, T. C., Eyring, V., Granier, C., Heil, A., Klimont, Z., et al. (2010). Historical (1850–2000) gridded anthropogenic and biomass burning emissions of reactive gases and aerosols: Methodology and application. *Atmospheric Chemistry and Physics*, *10*(15), 7017–7039. https://doi.org/10.5194/acp-10-7017-2010

McDougall, T. J., Jackett, D. R., Wright, D. G., & Feistel, R. (2003). Accurate and computationally efficient algorithms for potential temperature and density of seawater. *Journal of Atmospheric and Oceanic Technology*, *20*(5), 730–741. https://doi.org/10.1175/1520-0426(2003)20<730:aaceaf>2.0.co;2

Nakayama, Y., Menemenlis, D., Zhang, H., Schodlok, M., & Rignot, E. (2018). Origin of circumpolar deep water intruding onto the Amundsen and Bellingshausen Sea continental shelves. *Nature Communications*, *9*(1), 3403. https://doi.org/10.1038/s41467-018-05813-1

Pysarenko, L., Pishniak, D., & Savenets, M. (2023). Variability of extreme precipitation in West Antarctica and its response to the Amundsen Sea low changes. *Ukrainian Antarctic Journal*, *21*(27), 175–189. https://doi.org/10.33275/1727-7485.2.2023.716

Turner, J., Lu, H., King, J., Marshall, G. J., Phillips, T., Bannister, D., & Colwell, S. (2021). Extreme temperatures in the Antarctic. *Journal of Climate*, *34*(7), 2653–2668. https://doi.org/10.1175/jcli-d-20-0538.1

Vignon, É., Roussel, M.-L., Gorodetskaya, I., Genthon, C., & Berne, A. (2021). Present and future of rainfall in Antarctica. *Geophysical Research Letters*, *48*(8), e2020GL092281. https://doi.org/10.1029/2020gl092281

Wille, J. D., Favier, V., Gorodetskaya, I. V., Agosta, C., Kittel, C., Beeman, J. C., et al. (2021). Antarctic atmospheric river climatology and precipitation impacts. *Journal of Geophysical Research: Atmospheres*, *126*(8), e2020JD033788. https://doi.org/10.1029/2020jd033788